PROCEEDINGS OF SCIENCE

Investigation of Three-body Hadronic B decays at Belle

Min-Zu Wang[*†]
Department of Physics, Institute of Astrophysics and
Leung Center for Cosmology and Particle Astrophysics,
National Taiwan University, Taiwan
E-mail: `mwang@phys.ntu.edu.tw`

We investigate the three-body hadronic B decays using a large data sample collected by the Belle detector at the $\Upsilon(4S)$ resonance at the KEKB asymmetric energy e^+e^- (3.5 on 8 GeV) collider. These three-body decays include $B^0 \to D_s^- K_S^0 \pi^+$, $B^+ \to D_s^- K^+ K^+$ and $B^0 \to p\bar{\Lambda} D^{(*)-}$. Some useful information about the intermedidate two-body structure of these decays is addressed.

The European Physical Society Conference on High Energy Physics
22–29 July 2015
Vienna, Austria

*Speaker.
†on behalf of the Belle Collaboration

PoS(EPS-HEP2015)559

1. Introduction

Three-body B decays offer a good studying ground on the structure of the intermediate states with well developed techniques such as angular analysis or Dalitz analysis, etc.. For example, the exotic states like pentaquarks may be discovered in the 3-body baryonic B decays. Hadronic B decays are often used to check the interplay between the short-distance weak decay and the long-distance strong interaction/hadronization. It is known that the nonfactorizable effect can be well modeled by some universal parameters in the naïve or generalized factorization framework. Measurements of the decay branching fractions of various 3-body decay modes can be compared with the theoretical predictions. Last but not the least, measured branching fractions with similar decay diagrams can constrain the Cabibbo-Kobayashi-Maskawa (CKM) matrix elements which are the essential parameters in the Standard Model.

In this presentation, we report recent results related to three-body hadronic B decays, namely $B^0 \to D_s^- K_S^0 \pi^+$ [1], $B^+ \to D_s^- K^+ K^+$ and $B^0 \to p\bar{\Lambda} D^{(*)-}$. The data samples used contain $\sim 657 \times 10^6$ and $\sim 772 \times 10^6$ $B\bar{B}$ pairs collected by the Belle [2] detector at the $\Upsilon(4S)$ resonance at the KEKB [3] asymmetric energy e^+e^- (3.5 on 8 GeV) collider for $B^0 \to D_s^- K_S^0 \pi^+$ and $B^+ \to D_s^- K^+ K^+$, and $B^0 \to p\bar{\Lambda} D^{(*)-}$, respectively.

We use the silicon vertex detector and central drift chamber to determine the momenta of charged particles. The information gathered from the central drift chamber, aerogel threshold Cherenkov counters and time-of-flight scintillation counters can identify charged hadrons such as π^+, K^+ and p.

To extract signal yield, we use the following two kinematic variables: the energy difference $\Delta E = E_B - E_{\rm beam}$ and the beam-energy-constrained mass $M_{\rm bc} = \sqrt{E_{\rm beam}^2 - p_B^2 c^2}/c^2$, where E_B and p_B are the energy and momentum of the reconstructed B meson and $E_{\rm beam}$ is the beam energy, all measured in the $\Upsilon(4S)$ rest frame.

We generate signal and background (generic $B\bar{B}$ and continuum $e^+e^- \to q\bar{q}$) Monte Carlo (MC) samples in order to optimize the event selection criteria, obtain the distributions in ΔE and $M_{\rm bc}$ for both signal and background, and determine the signal efficiency.

2. $B^0 \to D_s^- K_S^0 \pi^+$ and $B^+ \to D_s^- K^+ K^+$ [4]

The leading decay diagram for $B^0 \to D_s^- K_S^0 \pi^+$ and $B^+ \to D_s^- K^+ K^+$ are shown in Fig. 1. The process $B^+ \to D_s^- K^+ K^+$ is Cabibbo suppressed in contrast to the Cabibbo favored $B^+ \to D_s^- K^+ \pi^+$. The ratio of the branching fractions of the above mentioned modes should be proportional to the ratio of the squares of the CKM matrix elements V_{ud} and V_{us} based on the naïve factorization picture [5].

We reconstruct the D_s^- candidates with all charged final-state particles (listed below): $\phi(\to K^+K^-)\pi^-$, $K^*(892)^0(\to K^+\pi^-)K^-$ and $K_S^0(\to \pi^+\pi^-)K^-$. We then perform unbinned extended maximum-likelihood fits to the $[\Delta E, M_{\rm bc}, M(D_s)]$ distributions of the selected candidate events in order to obtain the signal yields. Figure 2 shows the fit results of the $B^+ \to D_s^- K^+ K^+$ decay mode as an example. Assuming that the branching fractions of $\Upsilon(4S)$ decaying to the charged and neutral $B\bar{B}$ pairs are equal, we use the MC estimated efficiencies and fitted yields to determine:

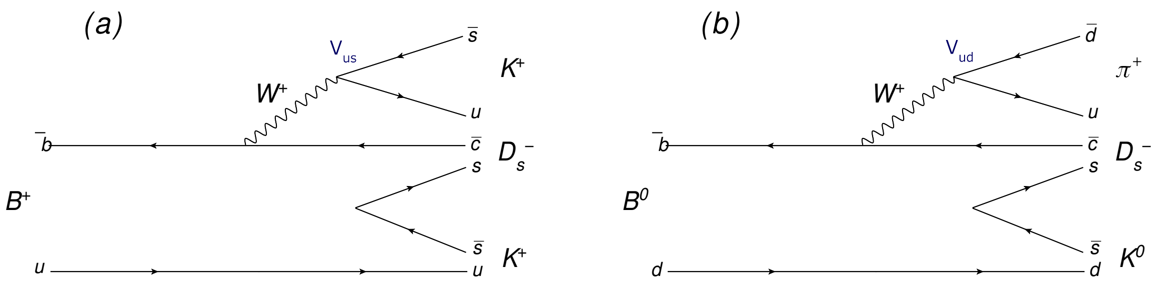

Figure 1: Dominant Feynman diagram for the (a) $B^+ \to D_s^- K^+ K^+$ and (b) $B^0 \to D_s^- K_S^0 \pi^+$ decay.

$$\mathscr{B}(B^0 \to D_s^- K_S^0 \pi^+) = [0.47 \pm 0.06(\mathrm{stat})\ \pm 0.05(\mathrm{syst})] \times 10^{-4}$$

and

$$\mathscr{B}(B^+ \to D_s^- K^+ K^+) = [0.93 \pm 0.22(\mathrm{stat}) \pm 0.10(\mathrm{syst})] \times 10^{-5}.$$

These values are consistent with, and more precise than, those reported by the BaBar Collaboration [6].

We also study the mass distribution of $D_s^- K_S^0$ ($D_s^- K_{\mathrm{low}}^+$) in $B^0 \to D_s^- K_S^0 \pi^+$ ($B^+ \to D_s^- K^+ K^+$), where K_{low}^+ denotes the kaon with the lower momentum. These distributions show a prominent peak near the the $D_s K$ mass threshold. More data are needed in order to perform a detailed angular analysis and ping down the nature of these structures.

Using the branching fraction obtained by Belle for the $B^+ \to D_s^- K^+ \pi^+$ decay [7], we calculate the ratio

$$\mathscr{R}_{\mathscr{B}} \equiv \frac{\mathscr{B}(B^+ \to D_s^- K^+ K^+)}{\mathscr{B}(B^+ \to D_s^- K^+ \pi^+)} = 0.054 \pm 0.013(\mathrm{stat}) \pm 0.006(\mathrm{syst}),$$

where the common systematic uncertainties cancel. This value is consistent with the theoretical expectation from the naïve factorization model,

$$\mathscr{R}_{\mathscr{B}}^{th} = \left(\frac{|V_{us}|}{|V_{ud}|}\right)^2 \cdot \left(\frac{f_K}{f_\pi}\right)^2 \cdot \frac{\mathscr{V}(D_s KK)}{\mathscr{V}(D_s K\pi)} = 0.066 \pm 0.001,$$

where f stands for the hadron decay constant and $\mathscr{V}$ represents the phase-space volume.

3. $B^0 \to p\bar{\Lambda}D^{(*)-}$ [8]

Based on the generalized factorization picture, baryonic B decays can be categorized into three different types: current, transition, and hybrid (containing both current and transition). Reference [9] predicts the following branching fractions

$$\begin{aligned}
\mathscr{B}(B^0 \to p\bar{\Lambda}D^-) &= (3.4 \pm 0.2) \times 10^{-6}, \\
\mathscr{B}(B^0 \to p\bar{\Lambda}D^{*-}) &= (11.9 \pm 0.5) \times 10^{-6}, \\
\mathscr{B}(B^+ \to p\bar{\Lambda}\bar{D}^0) &= (11.4 \pm 2.6) \times 10^{-6}, \\
\mathscr{B}(B^+ \to p\bar{\Lambda}\bar{D}^{*0}) &= (32.3 \pm 3.2) \times 10^{-6}.
\end{aligned}$$

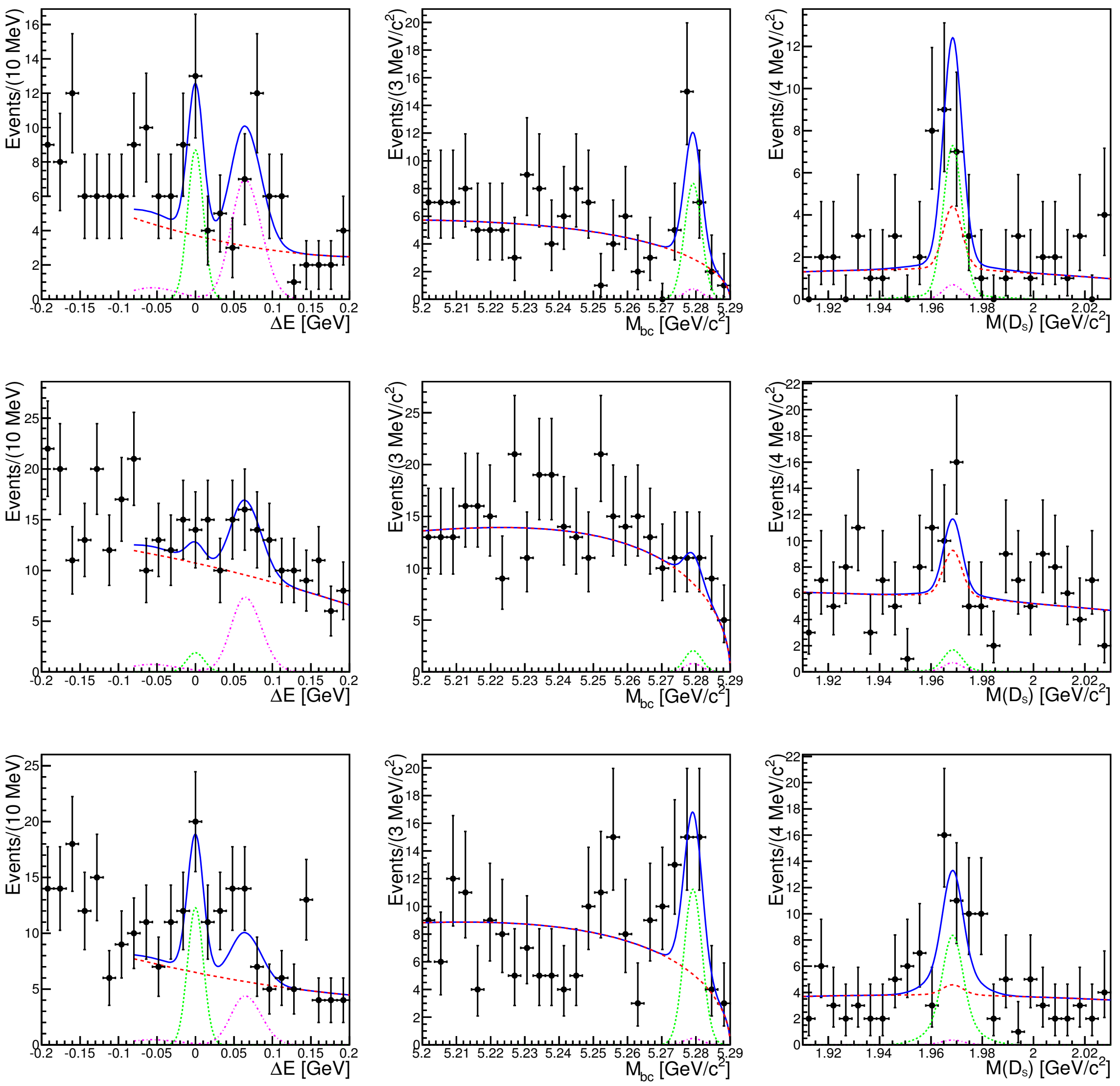

Figure 2: Distributions of ΔE, $M_{\rm bc}$ and $M(D_s)$ for (top) $B^+ \to D_s^-(\to \phi\pi^-)K^+K^+$, (middle) $B^+ \to D_s^-(\to K^{*0}K^-)K^+K^+$, and (bottom) $B^+ \to D_s^-(\to K_S^0 K^-)K^+K^+$ decays. The distribution for each quantity is shown in the signal region of the remaining two. The blue solid curves show the results of the overall fit described in the text, the green dotted curves correspond to the signal component, the red long-dashed curves indicate the combinatorial background (including the peaking D_s component) and the pink dot-dashed curves represent the $B \to D_s^{(*)} K\pi$ contribution.

The $B^0 \to p\bar{\Lambda}D^{(*)-}$ decay mode belongs to the current-type and its charged partner $B^+ \to p\bar{\Lambda}\bar{D}^{(*)0}$ is the hybrid-type. There are two interesting features of the predicted branching fractions. First, the ratios of the branching fractions of the decays into D^* to the analogous decays into D are $\approx 3:1$. Secondly, the branching fraction of the hybrid-type decay is also ≈ 3 times larger than the corresponding current-type decay. The measured branching fraction for $B^+ \to p\bar{\Lambda}\bar{D}^{(*)0}$ [10] is consistent with the theoretical calculation.

We reconstruct the $B^0 \to p\bar{\Lambda}D^{(*)-}$ signals through all charged final-state particles: $D^- \to$

$K^+\pi^-\pi^-$, $D^{*-} \to \bar{D}^0(\to K^+\pi^-)\pi^-$, and $\bar{\Lambda} \to \bar{p}\pi^+$. Using the signal and background distributions in ΔE and $M_{\rm bc}$, we perform unbinned extended maximum-likelihood fits to extract the signal yields in bins of $M_{p\bar{\Lambda}}$. The measured differential branching fractions are shown in Fig. 3. There are clear threshold enhancements in the mass spectra for both D ($B^0 \to p\bar{\Lambda}D^-$) and D^* ($B^0 \to p\bar{\Lambda}D^{*-}$) modes. The data are fitted with an empirical threshold yield, $m^a \times e^{(bm+cm^2+dm^3)}$, *vs.* the mass excess $m = M_{p\bar{\Lambda}} - M_{\bar{\Lambda}} - M_p$ by varying a, b, c, and d. The fit curves are overlaid in Fig. 3. We integrate the differential branching fractions over the full mass region in order to obtain:

$$\mathscr{B}(B^0 \to p\bar{\Lambda}D^-) = (25.1 \pm 2.6 \pm 3.5) \times 10^{-6},\ 19.8\sigma,$$

$$\mathscr{B}(B^0 \to p\bar{\Lambda}D^{*-}) = (33.6 \pm 6.3 \pm 4.4) \times 10^{-6},\ 10.8\sigma,$$

where the quoted uncertainties are statistical and systematic, respectively,

The measured branching fractions are much larger than the theoretical predictions for both the D and D^* modes. This indicates that some modifications are needed in the theoretical calculation.

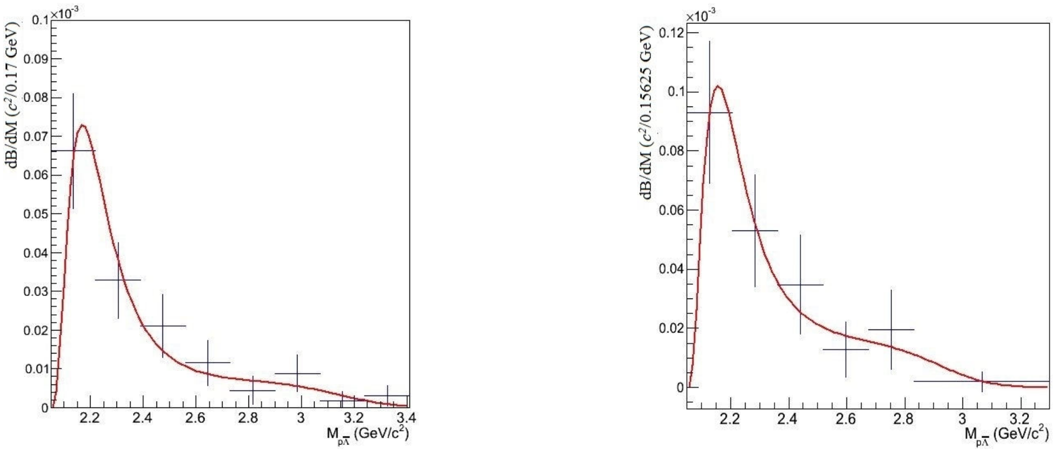

Figure 3: Differential branching fractions of the D (left) and D^* (right) modes in $M_{p\bar{\Lambda}}$. Fit curves are based on an empirical threshold function (see text).

To extract the decay angular distributions, we divide $\cos\theta_{pD^{(*)}}$ into eight bins, where $\theta_{pD^{(*)}}$ is defined as the angle between the proton and meson directions in the $p\bar{\Lambda}$ rest frame. Fig. 4 shows the measured results.

We define the forward-backward asymmetry $A_\theta = \frac{\mathscr{B}_+ - \mathscr{B}_-}{\mathscr{B}_+ + \mathscr{B}_-}$, where $\mathscr{B}_{+(-)}$ represents the branching fraction of positive (negative) cosine value. The results are

$$A_\theta(B^0 \to p\bar{\Lambda}D^-) = -0.08 \pm 0.10,$$

$$A_\theta(B^0 \to p\bar{\Lambda}D^{*-}) = +0.55 \pm 0.17,$$

The angular distributions of the D and D^* modes seem to have different trends. This may be interesting since they are both categorized as current-type decays. More data are needed to make the forward-backward asymmetry measurements more conclusive.

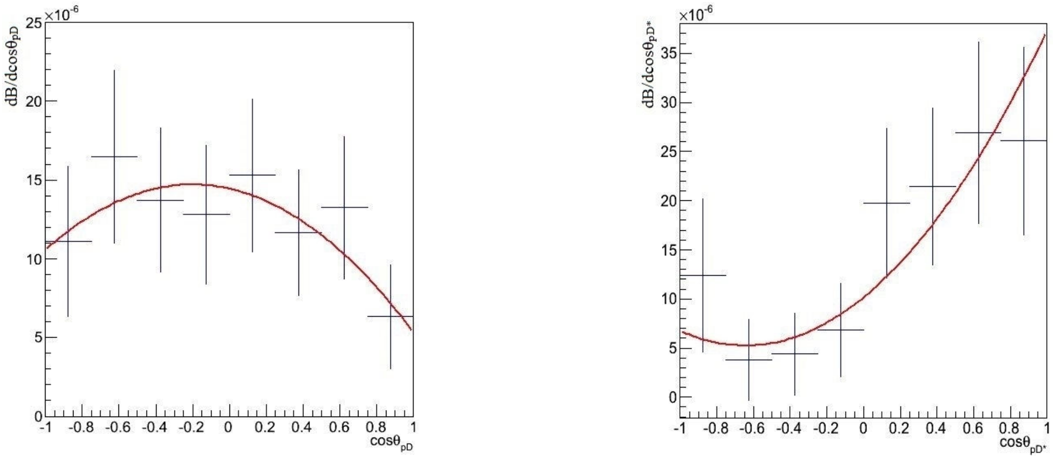

Figure 4: Differential branching fractions of the D (left) and D^* (right) modes in $\cos\theta_{pD^{(*)}}$. The fit curves are second-order polynomials, as suggested by Ref. [11].

Acknowledgments

The author wish to thank the KEKB accelerator group for the excellent operation of the KEKB accelerator. This work is supported by the Ministry of Science and Technology of the Republic of China under the grant MOST-103-2112-M-002-017-MY3.

References

[1] Throughout the paper, the inclusion of the charge-conjugate decay mode is implied unless otherwise stated.

[2] A. Abashian *et al.* (Belle Collaboration), Nucl. Instrum. Methods Phys. Res., Sect. A **479**, 117 (2002); also see the detector section in J. Brodzicka *et al.*, Prog. Theor. Exp. Phys. (2012) 04D001.

[3] S. Kurokawa and E. Kikutani, Nucl. Instrum. Methods Phys. Res. Sect., A **499**, 1 (2003), and other papers included in this Volume; T. Abe *et al.*, Prog. Theor. Exp. Phys. (2013) 03A001 and following articles up to 03A011.

[4] J. Wiechczynski *et al.* (Belle Collaboration), Phys. Rev. D **91**, 032008 (2015).

[5] M. J. Dugan and B. Grinstein, Phys. Lett. B **255**, 583 (1991).

[6] B. Aubert *et al.* (BaBar Collaboration), Phys. Rev. Lett. **100**, 171803 (2008).

[7] J. Wiechczynski *et al.* (Belle Collaboration), Phys. Rev. D **80**, 052005 (2009).

[8] Y.-Y. Chang *et al.* (Belle Collaboration), arXiv:1509:03034, to appear in Phys. Rev. Lett..

[9] C.Q. Geng *et al.*, Phys. Rev. D **78**, 054016 (2008).

[10] P. Chen *et al.* (Belle Collaboration), Phys. Rev. D **84**, 071501 (2011).

[11] C.Q. Geng and Y.K. Hsiao, Phys. Rev. D **74**, 094023 (2006).